Molecular Crystals and Liquid Crystals
Publication details, including instructions for authors and subscription information:
http://www.tandfonline.com/loi/gmcl16

Electrohydrodynamic Instabilities in Cholesteric Liquid Crystals with Negative Dielectric Anisotropy

H. Arnould-netillard [a] & F. Rondelez [a]
[a] Laboratoires d'Electronique et de Physique Appliquée, 3 av. Descartes, 94450, Limeil-Brevannes, (France)
Version of record first published: 28 Mar 2007.

To cite this article: H. Arnould-netillard & F. Rondelez (1974): Electrohydrodynamic Instabilities in Cholesteric Liquid Crystals with Negative Dielectric Anisotropy, Molecular Crystals and Liquid Crystals, 26:1-2, 11-31

To link to this article: http://dx.doi.org/10.1080/15421407408084820

Mol. Cryst. Liq. Cryst., 1974, Vol. 26, pp. 11-31

Printed in Dordrecht, Holland

Electrohydrodynamic Instabilities in Cholesteric Liquid Crystals with Negative Dielectric Anisotropy†‡

H. ARNOULD-NETILLARD and F. RONDELEZ

Laboratoires d'Electronique et de Physique Appliquée
3 av. Descartes, 94450 Limeil-Brevannes (France)

(*Received April 4, 1973*)

Electrohydrodynamic instabilities have been investigated in cholesteric liquid crystals with negative dielectric anisotropy. We have used a room-temperature mixture of nematic *p*-methoxy benzilidene *p-n* butyl aniline (MBBA) and cholesteryl nonanoate(CN). The ac electric field is applied parallel to the helical axis of the planar texture. The onset of a two-dimensional periodic pattern is optically observed at threshold. According to the excitation frequency, two regimes must be distinguished, namely a low frequency (conduction) regime and a high frequency (dielectric) regime. For both regimes, we give a full experimental analysis of the threshold voltage and of the period of the instability as a function of the various parameters (frequency, sample conductivity, cholesteric pitch, sample thickness). The dependence of the threshold conditions vs. frequency can be quantitatively accounted for by Hurault's theory in the low frequency regime. As far as the high frequency regime is concerned, no theory is available. It appears nevertheless that part of our results can be interpreted along the lines of the model developed by Dubois-Violette *et al.* for nematics. Finally, the behavior above threshold is briefly described.

INTRODUCTION

In nematics, electrohydrodynamic instabilities have been extensively studied by numerous workers and seem to be presently well understood at least at thres-

† Presented at the 4th International Liquid Crystal Conference – Kent (Ohio) – August 21-25, 1972

‡ Work partly supported by DRME under contract no. 72 34 208

hold.[1] When a voltage is applied across a thin layer of a nematic liquid crystal, the fluid is set into motion above a certain threshold. Systematic work has shown that under ac electric fields, the instability is caused by the Carr-Helfrich mechanism linked to the conductivity anisotropy. On the other hand, for dc applied fields, the instability is provoked by charge injection at the electrodes, a mechanism which is also present in isotropic liquids.[2]

An important effort has also been devoted to the behavior of cholesterics under applied electric fields. These studies were performed on cholesteric thin films sandwiched between two parallel semi-transparent electrodes.

Different types of effects were reported, depending on the orientation of the field with respect to the helical axis and also on the sign of the molecular dielectric anisotropy ϵ_a ($\epsilon_a = \epsilon_\parallel - \epsilon_\perp$), $\epsilon_\parallel$ and $\epsilon_\perp$ being the components of the dielectric susceptibility respectively parallel and perpendicular to the molecular axis.

For $\epsilon_a > 0$, a cholesteric to nematic transition has been observed by Wysocki *et al.*[3] and Baessler *et al.*[4] when the field is perpendicular to the helical axis. The unwinding of the cholesteric spiral has been calculated by Meyer[5] assuming a purely dielectric interaction between the applied field and the molecular dipole moment. His predictions have been verified very convincingly by Kahn.[6]

On the other hand, when the field is parallel to the helical axis Kahn[6] has also reported a 90° rotation of the helical axis. More recently, Gerritsma and van Zanten[7] have observed that the Grandjean planar texture could be distorted into a periodic cellular texture prior to the onset of a turbid aspect at higher excitation.

For $\epsilon_a < 0$, fewer results are available in the litterature. For cholesteryl nonanoate, Muller[8] has observed in dc and low frequency ac fields an increase in the intensity of the Bragg-scattered light by the periodic texture of the cholesteric mesophase. For cholesteric-nematic mixtures, the Xerox group[9] has also reported that (i) the original Grandjean planar texture, which is optically transparent, can be made scattering under low ac applied fields, (ii) the sample can then be cleared under high frequency (1 KHz) applied fields.

Another striking property of cholesterics under electric fields, is the existence of an optical storage effect, as first observed by Heilmeier[10] and later by many others.[9,11,12] This effect is found with both ϵ_a positive and negative. It was interpreted by Haas *et al.*[9,12] as a change from the planar texture to a light-scattering focal conic texture, due to electric fields. A recent parametric study of the life time of the memory effect has been made in our laboratory, by Hulin.[13]

To summarize, cholesterics can undergo a great variety of structural deformations under applied electric fields. However, for electric fields applied parallel to the helical axis, the stability conditions of the Grandjean planar texture were not clearly understood up to a recent period. In Ref. 14, Helfrich pointed out that,

in this geometry, a periodic bending mode could be nucleated at a low threshold field; such a sinusoïdal perturbation could be produced, either by a purely dielectric process[14] (i.e. with a magnetic analog) or by an electrohydrodynamic process[15] linked with material flow as shown in greater detail by Hurault.[16] This has indeed been observed by several authors. Rondelez and Arnould[17] have reported the onset of a grid like pattern in compounds with negative dielectric anisotropy which gives clear evidence of the electrohydrodynamic process. This process is also working in the experiments of Ref. 7 on materials with positive dielectric anisotropy as evidenced in a further publication by Rondelez, Arnould and Gerritsma.[18] On the other hand, Scheffer[19] and Rondelez and Hulin[20] have observed the same optical pattern in magnetic fields, showing the importance of the diamagnetic process.

These new results were obtained for two basic reasons:

– The experiments were performed on a well defined "monocrystalline" cholesteric planar texture,

– The materials used were nematic-cholesteric mixtures with large pitch values ($P \sim 10\ \mu$m). As a result, the sizes of the distorsions are larger: they can be observed in greater details and the threshold fields are smaller than in undoped conventional cholesterics.

The dependence of the threshold field and of the spatial periodicity of the distorsion with the geometrical characteristics of the system has been reported to be in agreement with Helfrich's predictions.[7,17-20] Moreover, the frequency dependence of the threshold conditions for a.c fields was studied in Ref. 18 with special emphasis on the low frequency ($f < 100$ Hz) region.

After the brief published reports on the basic phenomena, it seems desirable to present a detailed set of experimental observations on the electrohydrodynamic instabilities of a planar texture submitted to an electric field parallel to the helical axis. This is what we shall do in this communication, restricting our attention to materials with $\epsilon_a < 0$.

We limit also our study to ac excitations and shall not investigate the dc (or very low ac, $<$ 1Hz) case, since, as pointed out previously for nematics, charge injection effects may give rise to complications.

A detailed description of our experimental equipment is given in Section 2. In Section 3, we present our experimental results. The behavior at threshold induces us to define two regimes, the low frequency (or "conduction") and the high frequency (or "dielectric") one. The threshold characteristics (voltage and spatial periodicity of the distorsion) are studied versus the parameters of the system, the pitch P, the thickness L and the conductivity σ. In Section 4, we compare our results obtained at low frequencies with the recent predictions by Hurault. In the high frequency case, as no theoretical prediction is available yet,

our results are discussed within the framework of the theory for nematics. Finally, we describe our observations above threshold in Section 5 with emphasis on the existence of the memory effect.

EXPERIMENTAL EQUIPMENT

We use the same experimental set up as for nematics. An optical cell of variable thickness is made of two semi-transparent SnO_2-coated glass plates separated by mylar spacers (20–200 μm). The liquid crystal is introduced by capillarity between the two electrodes.

We observe the sample under a polarizing Leitz-orthoplan microscope in transmitted white light or monochromatic (sodium-5890 Å) light. Without further care, the field of view is invaded by numerous bundles of disclinations and the incident light is scattered, which gives a milky white aspect to the cholesteric layer. In order to get a uniform cholesteric planar (or Grandjean) texture with the helical axis perpendicular to the glass surfaces, a high voltage (300 V_{RMS}) and high frequency (1 000 Hz) ac field is applied for a few seconds. As first described by Haas *et al.*[9], the sample is cleared and the Grandjean planar texture is formed. Moreover, the molecular alignment at the glass boundaries can be imposed along a definite direction by the classical rubbing of the surfaces prior to filling the cell. The two rubbing directions are parallel in our experiments.

The homogeneity of the texture can be checked between polarizers because for $\lambda_{optical} \ll P \cdot \Delta n^{21}$ (Δn is the birefringence), the polarization of the incident parallel light beam follows adiabatically the helical twist. If the polarizer is set parallel to the rubbings, the light comes out linearly polarized in the same direction and can be fully extinguished if the analyser is crossed. In highly convergent light, a black cross characteristic of a uniaxial system with its axis along the viewing direction is observed for $P < 3$ μm. For higher P, the optical activity increases and the cross is smeared out. When existing, the introduction of a quarter-wave plate shows up a negative uniaxial interference figure as expected.

After a good planar texture is obtained, we apply an ac voltage to the electrodes. The range of frequency which has been investigated is 1 Hz–10 kHz with a maximum RMS value of 700 V. At threshold a pattern of bright optical lines is nucleated and is easily observed under the microscope.

The experiments reported here were carried out on mixtures of cholesteryl nonanoate (CN) and room temperature nematic *p*-methoxy benzilidene *p*-*n* butyl aniline (MBBA). The pitch P of that cholesteric material is adjusted by varying the relative mass concentration (C) of CN. In the low dilution regime $0 < C < 0.05$, PC is found to be a constant equal to 0.12 ± 0.01 μm. P is measur-

ed by confining the cholesteric compound between a half sphere lens and a plane microscope slide. We observe a series of concentric dark lines which are disclination lines. Their spacing is related to the pitch as discussed by Cano,[22] and, later, by the Orsay group.[23] The accuracy on pitch measurements is ± 2 μm.

For the low concentration of CN used, it will be assumed that the Frank elastic constants,[24] dielectric and diamagnetic constants are essentially the same as for undoped MBBA. There is some experimental evidence this assumption is correct. For example, the elastic constants determined in such mixtures are independent of C and are found to be the same as in undoped nematrics.[20] The actual values do not depend on the exact nature of the cholesterol esters used either.[25] Similar arguments seem also to hold in the case of the dielectric constant.

Thus we assume $\epsilon_a = \epsilon_\parallel - \epsilon_\perp$ as -0.5 where $\epsilon_\parallel$ and $\epsilon_\perp$ are measured parallel and perpendicular to the long molecular axis respectively and $\sigma_\parallel/\sigma_\perp = 1.5$.[26]

EXPERIMENTAL RESULTS

As pointed out previously, we have restricted our investigations to ac applied electric fields ($f > 1$ Hz) in order to avoid charge injection effects. We have also checked that our results could be reproduced using "blocking" electrodes (the SnO_2 semi-transparent electrodes being covered with thin layers of pyrex glass), which means that charge injection phenomena are not responsible for the instabilities we observe. Moreover, all the phenomena which are going to be described disappear above the cholesteric-isotropic transition temperature, evidencing that the effects are characteristic of the liquid crystal phase.

Under increasing fields, the optical appearance of the sample, which was initially transparent, is modified at a voltage V_{th} : at V_{th}, we detect the onset of a distortion pattern. We call V_{th} the optical threshold. As in nematics, we observe that the nature of the pattern depends upon the frequency f. This induces us to define two regimes, the low frequency regime ($f < f_c$), and the high frequency regime ($f > f_c$). The frequency f_c is called the cut-off frequency.

Low frequency

A static square grid pattern appears at V_{th}. Figure 1 displays a microphotograph of a typical sample illuminated with monochromatic light. The principal axes of that bi-dimensional figure are parallel and perpendicular to the rubbing direction. This regular array indicates that the unperturbed cholesteric planar texture undergoes two orthogonal periodic deformations. Due to the large optical birefringence ($\Delta n \simeq 0.2$), a small distortion of the molecular alignment induces a detectable change in the local refractive/index. The perturbed structure acts as

an array of lens. The bright lines are focals, as in nematics.[27] i.e. images of the light source located at the infinity and observed through the disturbed cholesteric layer. We can focus at different depths and obtain various optical patterns but without altering the aquare symmetry. When the polarization of the incident light is perpendicular to the rubbing direction, the optical pattern vanishes, indicating that the liquid crystal undergoes twist and/or bend deformations the axis of which are perpendicular to the helical axis.

Within experimental accuracy, the mesh of the pattern, Λ is independent of f up to f_c. The behavior of Λ with L and P has already been reported briefly in Ref. 17. More detailed data are displayed on Figure 2.

The threshold voltage V_{th} increases continuously with f. For $f < 0.9\, f_c$, V_{th} is slowly increasing with f. For $0.9 < f < f_c$, there is a sharp increase and V_{th} diverges for f_c. As observed in Ref. 18, f_c is proportional to the conductivity of the material. In Figure 3, V_{th} is plotted versus f for various pitches. f_c and L are identical in all three samples. The plot of V_{th} versus $L^{\frac{1}{2}}$ for various pitches is

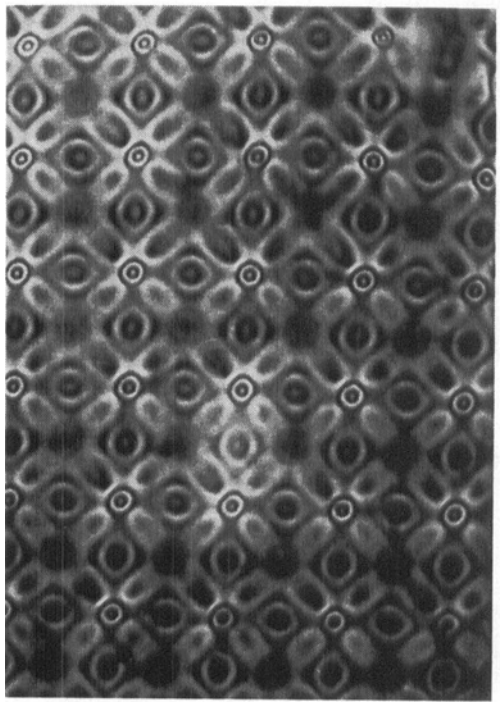

FIGURE 1 Conduction regime: typical microscopic appearance for a periodic two-dimensional distortion of the cholesteric planar texture under an ac electric field $\underset{\sim}{E}$. $\underset{\sim}{E}$ is applied parallel to the helical axis. MBBA + CN mixture; $P = 13\,\mu$m; applied voltage $\simeq 10\ V_{RMS}$; frequency = 3 Hz. The mesh of the square grid is 55 μm. Monochromatic (5890Å) light.

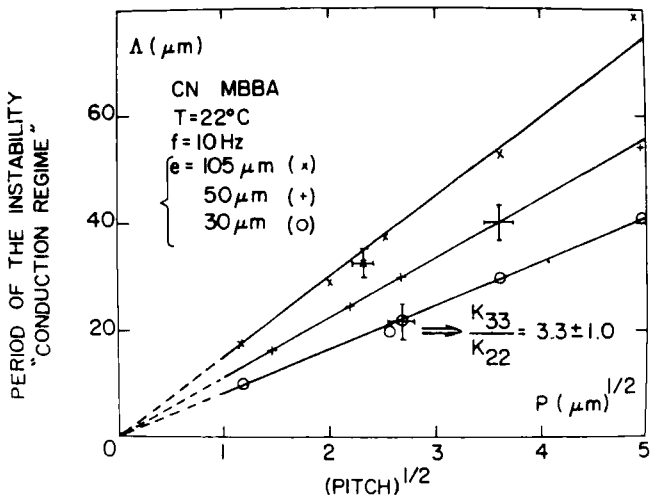

FIGURE 2 Conduction regime: period of the deformation at threshold vs. the square root of the pitch. The experimental points are given for several values of the sample thickness: 30, 50, 105 μm. MBBA + CN mixture; ac field frequency = 10 Hz. The straight lines stand for the theoretical predictions of Eq. (2) (see text).

given in Figure 4. The experimental accuracy on the determination of V_{th} is not better than 20% because V_{th} may vary locally in the sample from one region to another. This threshold behavior is strongly reminiscent of nematic liquid crystals apart from the fact that V_{th} was then independent of the sample thickness.

High frequency or "dielectric" regime

Beyond the cut-off frequency f_c, different types of optical patterns are observed at threshold. They are periodic and bi-dimensional with a square or an hexagonal symmetry. Figure 5 and Figure 6 display microphotographs taken in parallel white light and corresponding to different geometrical aspects. Opposite to the low frequency case, the distortions are not static but time-dependent as evidenced by a time recording of the transmitted light intensity. The intensity is modulated at twice the excitation-field frequency. For a sample of given P and L, the period Λ is also much shorter, typically in the few microns range. The voltage threshold V_{th} is again defined by the optical appearance of a regular pattern. This pattern is only visible if the polarizer is put parallel to the rubbing direction.

In Figure 7, we show measurements of the square of the threshold voltage as a function of frequency for various pitches. In the range of pitches under con-

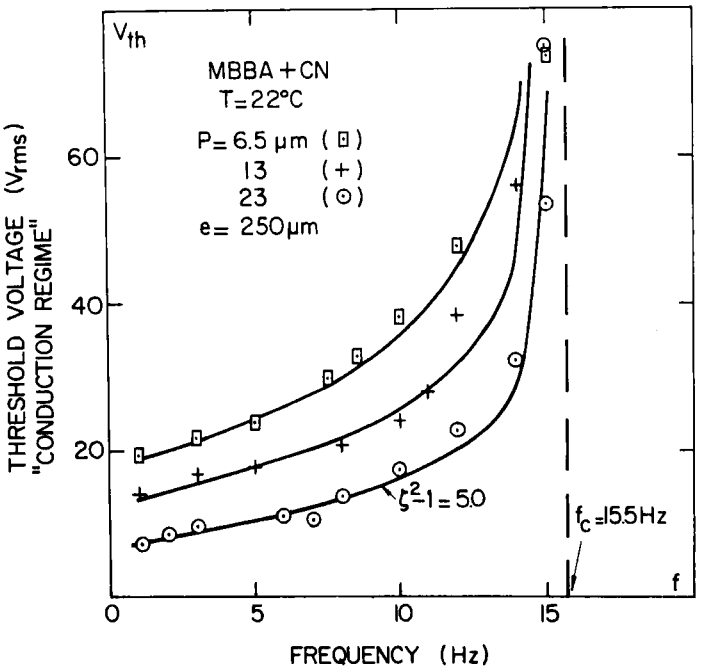

FIGURE 3 Conduction regime: threshold voltage vs. frequency of the electric field. The experimental points are given for $P = 6.5, 13, 23\,\mu$m. MBBA + CN mixture; sample tickness $= 250\,\mu$m. The solid lines stand for the theoretical predictions of Eq. (1) with a value of the parameter ζ^2-1 = 5.0 (see text). The curves diverge at the cut-off frequency $f_c = 15.5$ Hz, which is identical for all these samples.

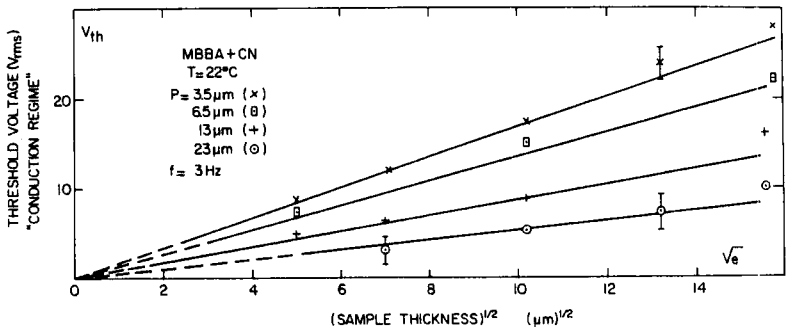

FIGURE 4 Conduction regime: threshold voltage vs. the square root of the sample thickness for several values of the cholesteric pitch $P = 3.5, 6.5, 13, 23\,\mu$m. MBBA + CN mixture; ac field frequency = 3 Hz. The straight lines stand for the theoretical predictions of Eq. (1) (see text).

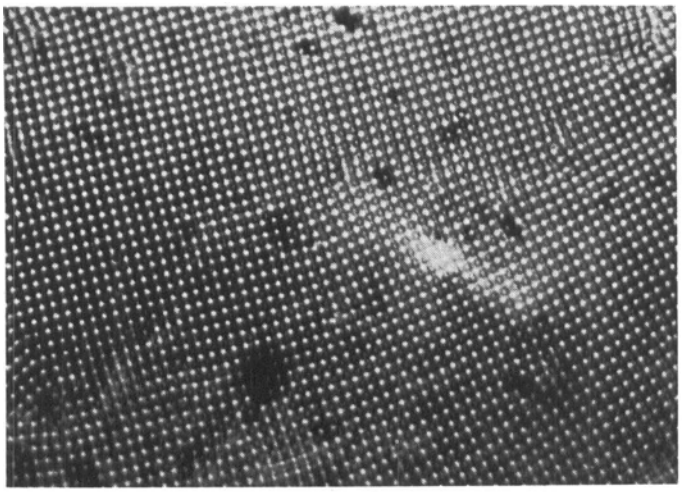

Fig. 5.

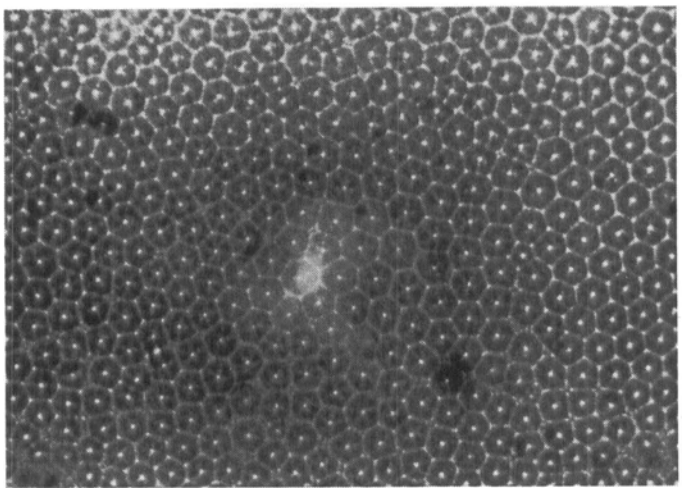

Fig. 6.

FIGURE 5 and 6 Dielectric regime: typical microscopie appearance of a periodic two dimensional distortion in a cholesteric planar texture under an ac electric field $\underset{\sim}{E}$. $\underset{\sim}{E}$ is applied parallel to the helical axis. MBBA + CN mixture; $P = 6.5\,\mu$m; sample thickness $= 100\,\mu$m.

Figure 5: Applied voltage $V = 149\ V_{RMS}$ Frequency = 100 Hz. Mesh of the pattern $= 4.2\,\mu$m

Figure 6: Applied voltage = 359 V_{RMS} Frequency = 600 Hz Mesh of the pattern = 12 μm

sideration, $3.7 < P < 13.0\ \mu m$, V^2_{th} is very weakly dependent on P. When P is infinite (undoped MBBA), V^2_{th} is decreased by a factor 2 as shown by the dotted line in Figure 7. The curves are linear so that V_{th} follows a parabolic law $V_{th} \sim f^{\frac{1}{2}}$. Varying the sample thickness, we find a field threshold: as in the dielectric regime for nematics, the voltages needed to nucleate the instabilities are proportional to L. By analogy, we shall call that high frequency instability for cholesteric liquid crystals, the "dielectric regime".

We shall turn now to a detailed description of the dependence of the distortion wavelength Λ as a function of the various parameters, namely L, P, f, f_c. As stated previously, Λ is small which does not allow for an easy observation at the microscope. To measure Λ more conveniently, we examine the diffraction pattern obtained with a laser beam impinging on the periodic array formed by the disturbed cholesteric texture. A parallel beam from a He-Ne laser ($\lambda = 6\,328$ Å) illuminates the cell perpendicular to the glass surfaces. On a screen 200 cm away from the cell, the Bragg scattered beams are observed as bright dots. From the scattering angle we derive the wavelength $q = \frac{2\pi}{\Lambda}$ of the distortion.

We have first studied Λ as a function of frequency. Let us consider a sample with $L = 50\ \mu m$ and $P = 7.5\ \mu m$ Figure 8 shows that the results depend strongly on actual value of the cut-off frequency f_c:

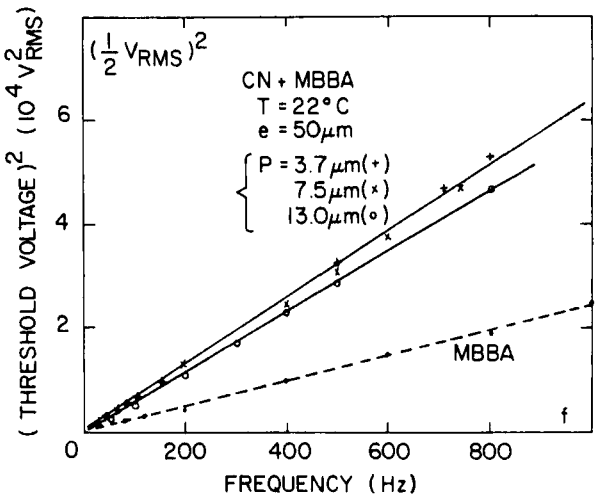

FIGURE 7 Dielectric regime: square of half the threshold voltage vs. frequency of the electric field. The experimental points are given for $P = 3.7$, 7.5, 13.0 μm and for infinite pitch (undoped MBBA). MBBA + CN mixture; sample thickness = 50 μm. The straight lines stand for $V_{th} \sim f^{\frac{1}{2}}$

i) if $f_c < 50$ Hz, the curve Λ versus f exhibits a minimum $\Lambda = \Lambda_{min}$ for a given frequency f_{min} which is close to f_c. At higher f, Λ reaches an asymptotic value which varies with f_c.

ii) if $f_c > 50$ Hz, decreases continuously with f, at least at threshold. The experimental law is found to be $\Lambda \sim f^{-\frac{1}{4}}$. Above threshold another deformation appears with a larger wavelength, as sketched by the arrows on Figure 8. We observed that Λ is then nearly constant with f.

Similar plots have been drawn for $P = 3.6$ μm, $L = 50$ μm, and $P = 14.5$ μm, $L = 100$ μm. A limiting value for the cut-off frequency has always been found:

$(f_c)_{limit} = 150$ Hz for $P = 3.6$ μm

$(f_c)_{limit} = 10$ Hz for $P = 14.5$ μm.

Above $(f_c)_{limit}$, we do not observe a minimum in the Λ vs. f curve any longer.

In the following, we shall discuss only the case $f_c < (f_c)_{limit}$. The strong frequency-dependence of Λ implies to specify both the frequency of the excitation field and the cut-off frequency f_c in any parametric study of Λ vs. L or P. The behavior of Λ versus L illustrates this fact very clearly. In Figure 9, we give a logarithmic plot of $\frac{2\pi}{\Lambda}$ versus L at two frequencies close and far from

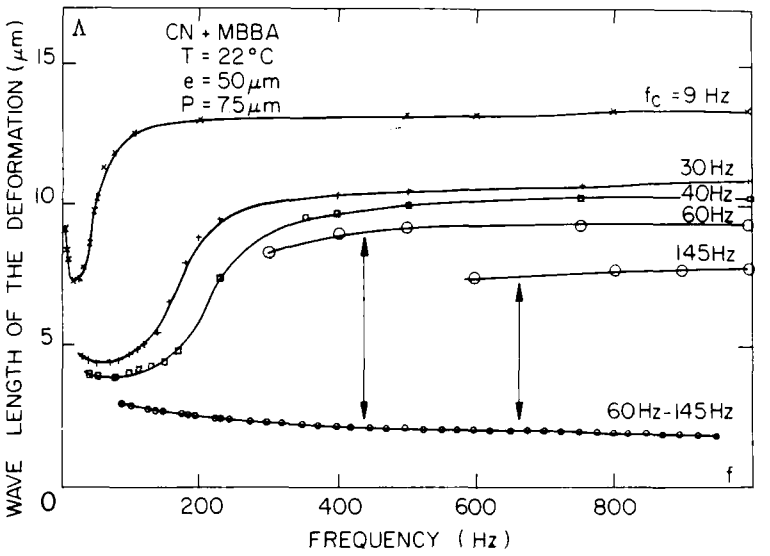

FIGURE 8 Dielectric regime: period of the distortion vs. frequency of the electric field. The experimental points are given for several values of the cut-off frequency $f_c = 9,30,40,60,145$Hz. MBBA + CN mixture; $P = 7.5$ μm; sample thickness = 50 μm. The solid lines are just a guide to the eye. The double arrows sketch the higher mode of instability observed above threshold when the Λ curve at threshold is decreasing monotonically (see text).

f_c ($\simeq$ 40Hz) respectively. All the experimental points correspond to samples with approximately the same f_c ($\simeq$ 40Hz). P is taken to be 3.6 μm and for that pitch value, a plot Λ vs. f for f_c = 40 Hz (not reported here) reveals that Λ has a minimum for f = 100 Hz. Figure 9 shows that for f = 100 Hz, Λ (= Λ_{min}) is independent of L whereas, for f = 500 Hz, Λ decreases as $L^{-\frac{1}{2}}$. We indeed observe quite different behaviors according to the excitation frequency f. Similarly, the P-dependence of Λ is dominated by the actual value of f_c. In the upper range of frequency ($f \simeq$ 500 Hz), Λ seems to be practically independent of P but is found to decrease linearly by a factor two when f_c increases from 30 to 90 Hz. In the lower range of frequency ($\simeq$ 100 Hz), Λ_{min} slightly increases with P : for f_c = 50 Hz, Λ_{min} is found to be 3 μm for P = 3 μm whereas it is equal to 6 μm

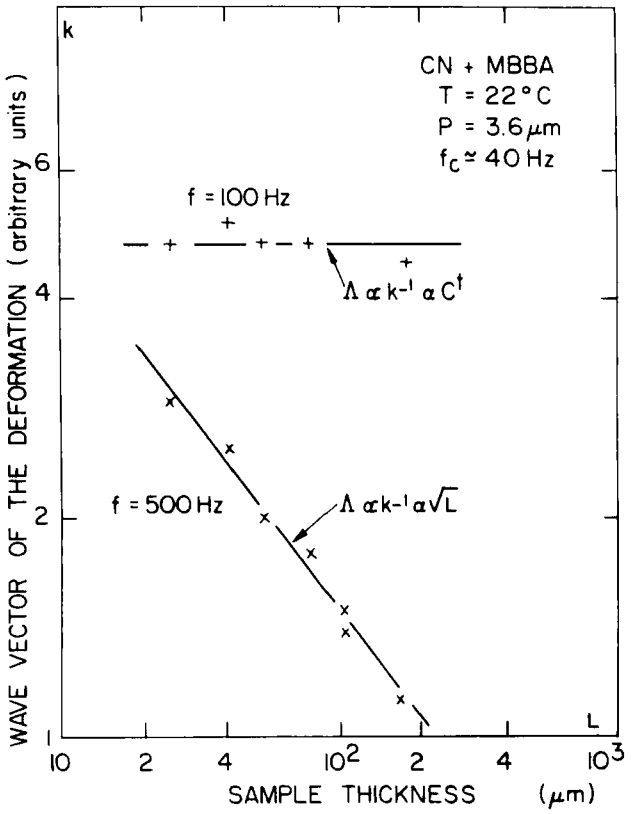

FIGURE 9 Dielectric regime: wave vector of the distortion vs. sample thickness in a log-log plot for two field frequencies. f = 100 Hz and f = 500 Hz. MBBA + CN mixture; p = 3.6 μm; $f_c \simeq$ 40 Hz. The solid lines correspond to $\Lambda = Ct$ and $\Lambda \sim L^{1/2}$ respectively.

for $P = 13\ \mu m$. On the other hand, Λ_{min} depends strongly on f_c. Figure 10 shows there is a linear relationship between Λ^2_{min} and $1/f_c$.

To summarize, the behaviors of Λ vs. f, vs. L and vs. f_c are indeed quite different according to the frequency range. These facts induce us to distinguish two different modes of hydrodynamic instabilities in the dielectric regime. These two modes cannot be distinguished from the analysis of the threshold behavior vs. frequency. They are revealed clearly by a plot of Λ versus the excitation frequency. If f_c is lower to a limiting frequency $(f_c)_{limit}$, which depends on the cholesteric pitch, there is one mode at low f and the other at higher f. If f_c is greater than $(f_c)_{limit}$, we observe just one mode of instability, at least at threshold.

DISCUSSION

The low frequency or conduction regime

In this regime, the observed distortion is static. Our observations can thus be compared to the predictions by Hurault, who has derived the threshold conditions for the onset of a static structural deformation under ac fields. In Ref. 16,

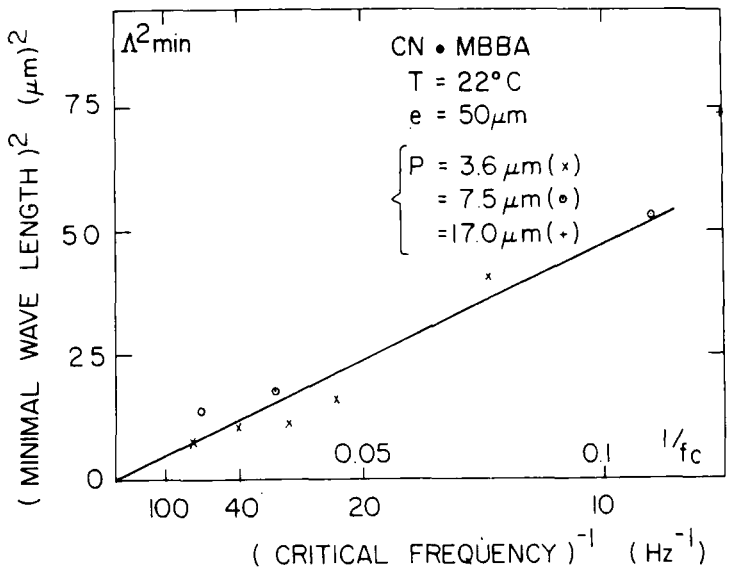

FIGURE 10 Dielectric regime: square of the minimum value for the period of the distortion versus the inverse of the cut-off frequency. The experimental points are given for $P = 3.6$, 7.5, $13\ \mu m$. MBBA + CN mixture; sample thickness $= 50\ \mu m$. The straight line stands for $\Lambda^2_{min} \sim f_c^{-1}$.

it has been found that an infinitesimal bend-and-twist mode of the cholesteric planes can be nucleated at a voltage V_{th} given by:

$$V_{th}^2 = \frac{8\pi^3}{\epsilon_\perp} \frac{\epsilon_\perp + \epsilon_\parallel}{\epsilon_\perp - \epsilon_\parallel} \frac{1 + \omega^2\tau^2}{\zeta^2 - 1 + \omega^2\tau^2} (\tfrac{3}{2}K_{22}K_{33})^{\frac{1}{2}} \frac{L}{P} \tag{1}$$

At threshold, the wavelength Λ of the deformation is given by

$$\Lambda^2 = \tfrac{3}{2}\left(\frac{K_{33}}{K_{22}}\right)^{\frac{1}{2}} PL \tag{2}$$

In (1) and (2), K_{22} and K_{33} are the Frank elastic constants for twist and bend respectively, ω is the pulsation of the excitation ($\omega = 2\pi f$); τ, the space charge relaxation time, is given by

$$\tau = \frac{1}{4\pi} \frac{\epsilon_\parallel + \epsilon_\perp}{\sigma_\parallel + \sigma_\perp} \tag{3}$$

$\sigma_{//}$ and $\sigma_\perp$ being the conductivities measured respectively parallel and perpendicular to the molecular axis. Finally, in (1), the dimensionless parameter $\zeta^2 - 1$ is given by

$$\zeta^2 - 1 = \frac{\sigma_\parallel - \sigma_\perp}{\sigma_\parallel + \sigma_\perp} \frac{\epsilon_\parallel + \epsilon_\perp}{\epsilon_\parallel - \epsilon_\perp} \tag{4}$$

When $\epsilon_a < 0$, V_{th} diverges for a critical frequency f_c given by

$$f_c = 2\sqrt{\zeta^2 - 1}\ \frac{\sigma_\parallel + \sigma_\perp}{\epsilon_\parallel + \epsilon_\perp} \tag{5}$$

As can be seen, the frequency dependence of the voltage conditions is very similar to the dependence derived for nematics in Ref. 1. This is due to the fact that, in the present case too, the Carr Helfrich mechanism (1) is basically responsible for the instability. However, compared to nematics, we can note the two following important differences:

– The cholesteric experiences a bending deformation coupled to a twisting deformation;

– The coefficient ζ^2 does not depend on any viscosity coefficient, whereas ζ^2, in nematics, depends upon a ratio of viscosity coefficients. This is due to the fact that, in the present case, the fluid motion takes place through permeation,[28] which implies that only one coefficient of viscosity will be dominant.

We shall now turn to compare quantitatively our experimental results with the above theoretical predictions.

As shown in Figure 2, Λ is indeed proportional to $(PL)^{\frac{1}{2}}$. This was also demonstrated in Ref. 17.

However the theoretical formula for Λ was wrong by a numerical coefficient; when the correction is made, we get from the slope of the curves:

$$\frac{K_{33}}{K_{22}} = 3.3 \pm 1.0 \quad \text{c.g.s.} \quad \text{at } 22°\text{C}$$

The experimental data for V_{th} as a function of f are in good agreement with the analytical form of Eq. (1). The best fit is obtained for $\zeta^2 = 6.0 \pm 1.0$. For the 250 μm sample of Figure 3, the solid curves represent Eq. (1) for various pitches assuming $\zeta^2 = 6$. If we compute ζ^2 from the data of the literature for undoped MBBA ($\sigma_\parallel / \sigma_\perp = 1.5$, $\epsilon_\perp = 5.2$, $\epsilon_\parallel = 4.7$ at 22°C), we find also $\zeta^2 = 6$.

As predicted by Eq. (1), V_{th} is found proportional to $(L/P)^{\frac{1}{2}}$ (see Fig. 4). From the slope of the curves V_{th} vs $L^{\frac{1}{2}}$ and taking $\zeta^2 = 6.0$, $\omega^2\tau^2 \ll 1$, one obtains:

$$K_{22}K_{33} = 33 \pm 8\times10^{-14} \text{ dyne}^2$$

Combining that data with our previous result for the ratio of the two elastic constants, this yields:

$$K_{22} = 3.3\times10^{-7}\text{dyne}$$
$$K_{33} = 10 \times10^{-7}\text{dyne}$$

The experimental accuracy on these data is not better than 50%. Our determination of K_{22} and K_{33} yields the correct order of magnitude and is in relatively good agreement with other data published in the literature.[29]

To conclude with the conduction regime, the static deformation of the cholesteric planes which is nucleated at threshold by the electrohydrodynamic instabilities seem to be presently well understood experimentally and Hurault's theory allows for a quantitative understanding of the complete set of our results.

The high frequency or "dielectric" regime

In opposition to the previous case, no theory for the high frequency regime has been published so far for cholesterics.

As in nematics above f_c,[1] we have to deal with a time dependent periodic orientation of the molecular director. But the situation is more complex here because a time dependent twisting mode will be associated to a time dependent bending mode. On the other hand, it has been shown [30] that the twist deformation cannot follow the excitation beyond a critical frequency f_t given by

$$f_t = \frac{2\pi K_{22}}{\gamma_1 p^2}$$

γ_1 being the shear viscosity.

For $P = 3\ \mu m$, $\gamma_1 = 1.2\ P$;[31] at 22°C, $f_t = 17$ Hz.

Thus, the observations should be qualitatively different when $f < f_t$ or when $f > f_t$.

On the other hand, by analogy with nematics, we also expect that the wavelength of the distortion cannot be less than the Debye radius for a local fluctuation in the charge density, Λ_D. If Λ becomes of the order of Λ_D, diffusion currents become important. This effect has been fully analyzed by Dubois Violette who makes two predictions:[32]

1) Λ should present a minimum value Λ_{min} proportional to Λ_D for a frequency f_{min};

2) f_{min} is related to the conductivity (or to the cut-off frequency f_c) by a linear equation. The coefficient of proportionality depends on the elasticity and viscosity coefficients.

The experimental evidence of the theory in the nematic phase has been reported by Galerne, Durand and Veyssié for MBBA.[33]

Figures 10 and 11 show our results in the case of cholesterics. We have plotted in Figure 10 the dependence of Λ^2_{min} versus the inverse of the cutt-off frequency,

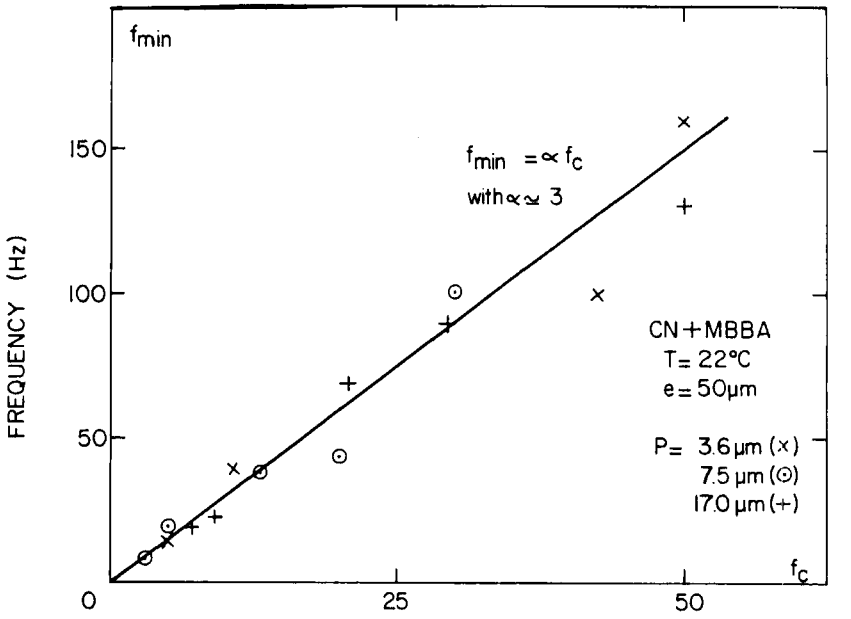

FIGURE 11 Dielectric regime: frequency at which the period of the distortion is minimum, f_{min}, versus the cut-off frequency. The experimental points are given for $P = 3.6$, 7.5, 17.0 μm. MBBA + CN mixture, sample thickness = 50 μm. The straight line stands for $f_{min} = \alpha f_c$ with $\alpha = 3$.

f_c^{-1}. We get a linear relation, as expected because $\Lambda_D^2 \propto \sigma^{-1} \propto f_c^{-1}$ (σ is an average conductivity). In first approximation, the slope of the theoretical straight line does not seem to be dependent on the actual pitch of the material. In Figure 11, we have plotted f_{min} versus f_c. Again, we obtain a linear relationship, independent of the pitch: $f_{min} = \alpha f_c$. The coefficient α is found to be $\sim 3 (\alpha \sim 7$ for MBBA[33]). So, as far as the existence of a minimum value for Λ is concerned, it seems likely to be due to diffusion currents as in nematics. However, we cannot explain yet why no minimum is observed when $f_c > (f_c)_{limit}$.

In the upper frequency range, a new mode of instability occurs, as evidenced by the quite different behavior with the sample thickness (see 3.2). It is tempting to relate f_{limit} the frequency limit between the two modes in the dielectric regime, to f_t where the twist angle cannot follow the excitation any longer. Varying the pitch P between 3.6 and 13 μm, we do observe that f_{limit} decreases when P increases: f_{limit} = 300-200-50Hz for P = 3.6-7.5-13μm. However the uncertainty on the determination of f_{limit} is too large to make a quantitative check with a P^{-2} law. Moreover, f_{limit} depends on f_c and changes by a factor 2 with f_c varying between 10 and 60 Hz (see Figure 8). Thus, in this latter case, we are unable to propose any quantitative interpretation of our observations. This can however be compared to the case of nematics where a similar very high frequency mode has also been detected,[33] without having received any interpretation either.

To summarize, the dielectric regime is characterized by several modes of distorsion, the properties of which are very different from one another there is some evidence of a similarity with what has been found in nematics, it is not presently possible to draw a definite scheme of the electrohydrodynamic instabilities in that regime.

BEHAVIOR ABOVE THRESHOLD

When the applied voltage is increased above the threshold, very spectacular effects are observed.

In the conduction regime, the square grid pattern is progressively replaced by a new structure which is nucleated from the centres of the squares. Double spirals of bright lines are formed and extend to the whole sample area when the voltage is further increased (typically for $V = 2\text{-}3\ V_{th}$). As already noticed[17] the spatial periodicity is equal to $P/2$ indicating the helical axis has been tilted by 90° and is now perpendicular to the electric field. The new tilted structure is very regular as can be seen in Figure 12. This cholesteric arrangment has been recently described by Bouligand.[34] It corresponds to the so-called polygonal textures. Two sets of spirals must be distinguished: the ones surrounding the centres of the previous squares and those surrounding their tops. They are left

and right handed respectively; this is in agreement with the observations of Bouligand. Moreover the structure at the centres of the squares is related to the chirality of the cholesteric mesophase. In the case of MBBA + CN mixtures, the cholesteric liquid crystal is found to be left handed, as for all cholesterol esters.

When the excitation is released, that titled structure is metastable and relaxes to the planar texture within a time τ. A parametric study of τ as a function of L and P has been recently reported by Hulin.[13] It can reasonably be assumed that the memory effect for cholesterics[10] is due to the tilting over of the initial planar texture under the influence of an electric field.

Under still increasing fields, the dynamic scattering mode sets up. The flow becomes turbulent and the molecular alignment is strongly perturbed. The dust particles suspended in the liquid crystal move very quickly and in a random manner. No regular optical pattern can be observed any more. However for very high voltages (> 300 V) the turbulent motion is sometimes established within a

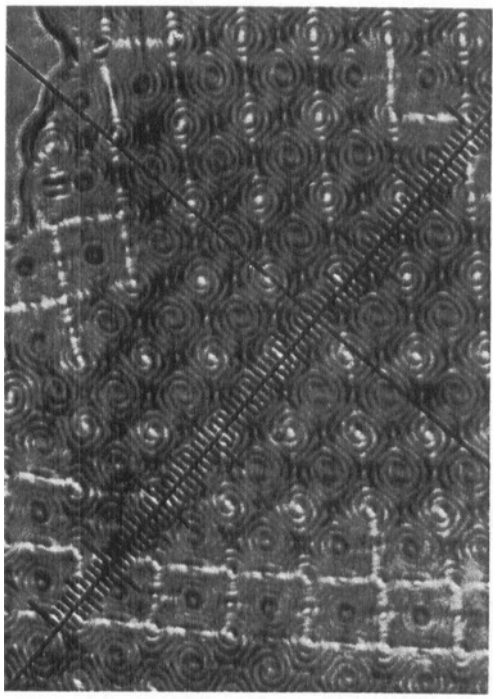

FIGURE 12 Conduction regime: typical microscopic appearance of the pattern observed above threshold. This titled structure is responsible for the memory effect in cholesterics. MBBA + CN mixture; $P = 7.5\ \mu$m; sample thickness $= 25\ \mu$m. Applied voltage $= 16\ V_{RMS}$, $f = 6$ Hz (threshold voltage $= 6\ V_{RMS}$). The square grid can still be distinguished. Mesh of the square grid $= 22.4\ \mu$m.

quite regular grid-like pattern (Figure 13) of periodicity Λ_{DSM}. A dust particle in a given square cell will move periodically from the tops of the square up to the centre, which gives the dark lines at 45° from the square-edges on the micro-photographs. A certain regularity in the fluid flow has also been observed in nematics by Gruler and Meier.[35] The period Λ_{DSM} is found to be related to the period of the grid pattern in the conduction regime and not to the sample thickness alone as it could have been expected. It indicates the regularity observed in the turbulent regime is due not only to the boundary conditions (on the glass surfaces, the normal component of the fluid velocity must be equal to zero) but also to more "microscopic" conditions related to the pitch of the cholesteric sample. This periodic turbulent mode of instability is observed as well in the conduction regime as in the dielectric regime. There is no apparent discontinuity in the optical observations when crossing the cut-off frequency f_c between the two regimes.

In the dielectric regime, we reported in Section 3.2 that 10-20 V above

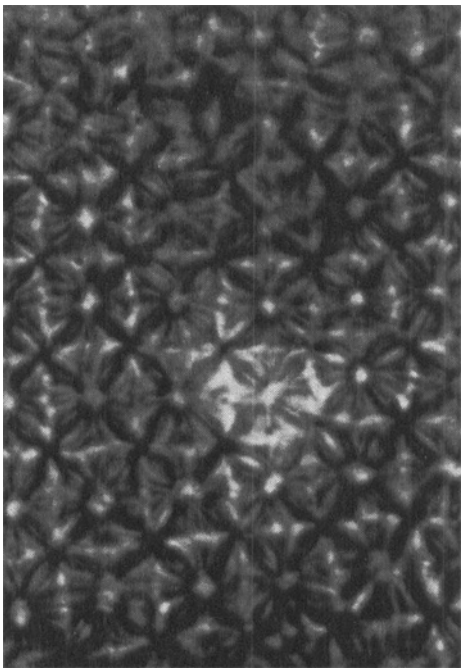

FIGURE 13 Optical transmission pattern of the periodic cellular structure which appears in the turbulent regime. MBBA + CN mixture; $P = 3.5\,\mu m$; sample thickness = $50\,\mu m$; applied voltage = 490 V_{RMS}; $f = 300$ Hz ($f_c = 30$ Hz). Mesh of the square grid = $30\,\mu m$ (the mesh in the conduction regime is 21 μm).

threshold, a sudden change in the wavelength of the deformation sometimes occurs. This effect has still to be investigated.

CONCLUSION

There is now clear experimental evidence for electrohydrodynamic effects in cholesteric liquid crystals. Since the first report by Muller, the use of monocrystalline, larger pitch samples, has given rise to controllable and reproducible results. The Carr-Helfrich mechanism seems to be basic for the onset on instabilities as in nematics. As far as the stability conditions of the planar cholesteric texture are concerned, a quantitative understanding has been achieved for the static distorsions which appear for $\epsilon_a < 0$ under a critical frequency f_c. For $f > f_c$, our observations can be roughly explained using some concepts which were developed in nematics. However, a unified theory of these effects is not available yet.

References

1. For reference papers see for instance: Orsay Liquid Crystal Group, *Mol. Cryst. and Liq. Cryst.* **12**, 251 (1971); Dubois-Violette, E., de Gennes, P. G. and Parodi, O., *J. Phys.* 305 (1971).
2. Felici, N., *Direct Current* **2**, 147 (1972).
3. Wysocki, J., Adams, J. and Haas, W., *Phys. Rev. Letters* **20**, 1024 (1968).
4. Baessler, H. and Labes, M. M., *Phys. Rev. Letters* **21**, 1971 (1968).
5. Meyer, R. B., *Appl. Phys. Letters* **12**, 281 (1968).
6. Kahn, F. J., *Phys. Rev. Letters* **24**, 209 (1970).
7. Gerritsma, C. J. and van Zanten, P., *Phys. Letters* **37A**, 47 (1971).
8. Müller., J. H., *Mol. Cryst.* **2**, 167 (1966).
9. Haas, W., Adams, J. and Flannery, J. B., *Phys. Rev. Lett.* **24**, 577 (1970).
10. Heilmeier, G. H. and Goldmacher, S. E., *Appl. Phys. Letters* **13**, 132 (1968).
11. Melamed, L. and Rubin, D., *Appl. Phys. Letters* **16**, 149, (1970).
12. Haas, W., Adams, J. and Dir, G., *Chem. Phys. Letters* **14**, 95 (1972).
13. Hulin, J. P., *Appl. Phys. Letters* **10**, 455 (1972).
14. Helfrich, W., *Appl. Phys. Letters* **17**, 531 (1970).
15. Helfrich, W., *J. Chem. Phys.* **55**, 839 (1971).
16. Hurault, J. P., to appear in *J. Chem. Phys.* (August 1973)
17. Rondelez, F. and Arnould, H. *C.R. Acad. Sci.* (Paris) **273B**, 549 (1971).
18. Rondelez, F., Arnould, H. and Gerritsma, G. J., *Phys. Rev. Letters* **28**, 735 (1972).
19. Scheffer, T. J., *Phys. Rev. Letters* **28**, 593 (1972).
20. Rondelez, F. and Hulin, J. P., *Solid State Comm.* **10**, 1009 (1972).
21. Mauguin, C. *Bull. Soc. Franç. Mineral. Crist.* **34**, 3 (1911).
22. Cano, R., *Bull. Soc. Franç. Mineral. Crist.* **91**, 20 (1968).
23. Orsay Liquid Crystal Group, *Phys. Letters* **28A**, 687 (1969).
24. Frank, F. C., *Disc. Faraday Soc.* **25**, 19 (1958).
25. Durand, G., Léger, L., Rondelez F. and Veyssié, M., *Phys. Rev. Letters* **22**, 227 (1969).
26. Diguet, D., Rondelez, F. and Durand, G., *C.R. Acad. Sci.* (Paris) **271B**, 954 (1970).
27. Durand, G. M., Veyssié, M. F., Rondelez, F. and Léger,L., *C.R. Acad. Sci. (Paris)* **270B**, 97 (1970).

28. Helfrich, W., *Phys. Rev. Letters* **23**, 372 (1969).
29. See for example: Haller, I., *J. Chem. Phys.* 57, 1400 (1972); also Ref. 20.
30. Fan, C., Kramer, L. and Stephen, M., *Phys. Rev.* **2A**, 2482 (1970).
31. Prost, J. and Gasparoux, H., *Phys. Letters* **36A**, 245 (1971).
32. Dubois-Violette, E., Thesis, Orsay 1971, unpublished.
33. Galerne, Y., Durand, G. and Veyssié, M., *Phys. Rev.* **6A**, 484 (1972).
34. Bouligand, Y., *J. Phys.* **33**, 715 (1972).
35. Gruler, H. and Meier, G., *Mol. Cryst.* a *Liq. Cryst.* **12**, 289 (1971).